Effect of Sodium Citrate and Urea as Additive on the Synthesis of Hydroxyapatite from Blood Cockle Shells: Kinetics and Adsorption Isotherms Study of Coomassie Brilliant Blue

Dhea Rahmanda Putri[1], Novesar Jamarun[1*], Upita Septiani[1], and Vivi Sisca[2]

[1]*Department of Chemistry, Faculty of Mathematics and Natural Sciences, Universitas Andalas, Limau Manis, Padang 25163, Indonesia*

[2]*Research Center for Chemistry, National Research and Innovation Agency (BRIN), KST BJ Habibie, Setu, Tangerang Selatan 15314, Indonesia*

* ***Corresponding author:***

tel: +62-8126713521
email: novesarjamarun@sci.unand.ac.id

Received: December 11, 2024
Accepted: May 1, 2025

DOI: 10.22146/ijc.102465

Abstract: *Hydroxyapatite (HAp) was synthesized from blood cockle shell waste by the sol-gel method, incorporating sodium citrate and urea as additives for Coomassie brilliant blue (CBB) adsorption. The synthesis included HAp without additives (HAp 1) and with 30 g/L of urea and varying sodium citrate concentrations of 0 (HAp 2), 0.1 (HAp 3), 0.2 (HAp 4), 0.3 (HAp 5), 0.4 (HAp 6), and 0.5 (HAp 7) g/L. HAp 4 showed the highest adsorption capacity at 96.60 mg/g. FTIR analysis of HAp 4 revealed adsorption bands for O–H and PO_4^{3-} groups. XRD analysis indicated a crystal size of 24.55 nm with low crystallinity. SEM-EDS analysis showed a Ca/P ratio of 1.28, with an irregular shape due to agglomeration and an average particle size of 1.16 μm. SAA analysis found a surface area of 107.18 m^2/g, a pore size of 12.55 nm, and a pore volume of 0.36 cm^3/g. HAp 4 followed the Langmuir and pseudo-second-order isotherm models in CBB adsorption and demonstrated five-time reusability, proving it to be an effective adsorbent for CBB dyes.*

Keywords: *hydroxyapatite; sodium citrate; urea; adsorption; Coomassie brilliant blue*

■ INTRODUCTION

The use of synthetic dyes in the textile and food industries has rapidly increased with the development of modern industry. Industrial growth in Indonesia has a significant positive impact on the country's economy. With its extensive use of dyes and chemicals, the textile industry stands out as a significant source of water pollution [1]. The dyes used in these industries are highly diverse and typically consist of various coloring agents. Excessive use of these dyes can harm human health and aquatic life [2].

Coomassie brilliant blue (CBB) is one of the most used synthetic dyes and significantly contributes to wastewater pollution. These toxic dye molecules cause ecosystem imbalance and potential health risks to humans and exposed organisms [3]. Efforts to mitigate the negative impacts of synthetic dyes have become a major focus of research across various fields. One promising approach is the development of effective adsorbent materials to capture and remove synthetic dyes from wastewater [4].

Hydroxyapatite (HAp) is a calcium phosphate-based biomaterial with the chemical formula of $Ca_{10}(PO_4)_6(OH)_2$, used in various fields such as medicine, biotechnology, and as an adsorbent in wastewater treatment [5]. HAp as an adsorbent is growing, particularly in addressing household and industrial waste pollution. HAp can be obtained from natural materials such as cuttlebones, abalone shells, egg shells, blood cockle shells, and fish bones [5-9]. In this study, blood cockle shells, rich in calcium carbonate ($CaCO_3$), serve as the Ca source in HAp synthesis. Blood cockle shells contain 98.7% $CaCO_3$. Utilizing blood cockle shells as a source of calcium oxide (CaO) for HAp synthesis represents an effort to valorize fishery waste and an alternative solution to the limited availability of HAp [8].

Previous research has shown that sodium citrate and urea can influence the morphology of HAp. The morphology of HAp significantly impacts pore size, shape, and specific surface area, which are related to its adsorption capacity. Sodium citrate is as an additive and stabilizing agent due to its good biocompatibility and strong binding ability with calcium ions. Sodium citrate and urea significantly influence the pore size, shape, and surface area of HAp through their chemical structures and behaviors during the synthesis process. Sodium citrate, with its three carboxylate groups, acts as a potent chelating agent by binding Ca^{2+} ions in the solution. This chelation slows the release of free Ca^{2+}, thereby controlling the nucleation and growth of HAp crystals. As a result, the particles formed are smaller, more uniform, and exhibit higher surface area.

Additionally, sodium citrate can adsorb onto specific crystal faces, inhibiting growth in certain directions and leading to variations in crystal shape, such as rods, needles, or plates. Upon calcination, the decomposition of organic citrate residues also contributes to pore formation, increasing the material's porosity and average pore size. Several studies have shown that using sodium citrate in HAp synthesis can enhance the adsorption capacity for various dyes. For example, HAp synthesized with sodium citrate improves dye removal performance [10-11].

Meanwhile, urea slowly hydrolyzes upon heating to release ammonia (NH_3) and carbon dioxide (CO_2). The gradual release of NH_3 raises the pH of the solution steadily, promoting a uniform and controlled precipitation of HAp. This results in a narrower particle size distribution and enhances surface area. Furthermore, the CO_2 gas evolved during urea decomposition can create physical pores within the HAp structure, contributing to mesoporosity or even macroporosity depending on the synthesis conditions. Altogether, the presence of sodium citrate and urea in the synthesis system facilitates the formation of HAp with tailored porosity, morphology, and improved surface characteristics, which are critical for applications like drug delivery, catalysis, or bone tissue engineering [10-13].

Thus, this research presents an innovation in synthesizing HAp from cockle shells with the combined addition of sodium citrate and urea, which further aims to improve the material's structural and adsorption properties. The novelty lies in the variation of sodium citrate concentrations used and the incorporation of urea as an additional morphology-directing agent. These modifications have not been comprehensively studied in previous works. This study not only contributes to enhancing the adsorption capacity of HAp for CBB dye but also supports the valorization of natural waste materials and offers a sustainable approach to wastewater pollution problems.

■ EXPERIMENTAL SECTION

Materials

The materials used in this study include CaO powder from blood cockle shell waste from the coast of Padang, West Sumatra, acetic acid (CH_3COOH, Merck), disodium hydrogen phosphate hydrate ($Na_2HPO_4{\cdot}12H_2O$, Merck), sodium citrate hydrate ($C_6H_5Na_3O_7{\cdot}H_2O$, Merck), urea (H_2NCONH_2, Merck), sodium hydroxide (NaOH, Merck), hydrochloric acid (HCl), deionized water, ethanol, CBB G 250 (Merck), and Whatman No. 42 filter paper.

Instrumentation

The equipment used in this study includes a mortar, pestle, grinder (Fritsch Pulverisette 16), furnace (Thermo Insight), hot plate, magnetic stirrer, analytical balance, aluminum foil, oven (Labtech), universal pH paper, and glassware. The characterization tools used are Fourier transform-infrared (FTIR spectrometer Frontier PerkinElmer), X-ray diffraction (XRD, PANalytical X'Pert PRO), scanning electron miscrocope-energy dispersive X-ray spectroscopy (SEM-EDS, Thermofisher Quattro S), surface area analyzer (SAA, TriStar II Plus Version 3.01), and UV-vis spectrophotometer (Genesys 20 Thermo Scientific).

Procedure

Synthesis of HAp using the sol-gel method

The synthesis of HAp is performed using CaO from the blood cockle shells and CH_3COOH via the sol-

gel method. First, 1.09 g of CaO powder is dissolved in 35 mL of 2 M CH_3COOH, stirred at 65 °C for 30 min at 250 rpm, and then filtered. The filtrate is titrated with 10 M NaOH dropwise until pH 11 is reached. The resulting sol ($Ca(OH)_2$) is then mixed with 4.1899 g of $Na_2HPO_4{\cdot}12H_2O$ dissolved in 65 mL distilled water, drop by drop. $C_6H_5Na_3O_7{\cdot}H_2O$ and urea H_2NCONH_2 are added to the HAp sol in varying concentrations as shown in Table 1 and stirred for 3 h. The resulting gel is cooled at room temperature and filtered. The filtrate is discarded, and the precipitate is dried at 110 °C for 5 h. The HAp is then washed several times with distilled water and ethanol and calcined at 600 °C for 3 h [10].

Characterization of HAp

HAp characterization is performed using instruments including FTIR, XRD, SEM-EDS, and SAA. FTIR characterization identifies chemical bonds and functional groups in HAp. XRD characterization detects and analyzes the crystal structure of the synthesized HAp. SEM-EDS characterization examines surface morphology and determines the Ca/P ratio of the product. SAA characterization measures the surface area, pore size, and pore volume of HAp.

Determination of adsorption capacity of HAp from blood cockle shells

HAp from blood cockle shells is tested for its adsorption capacity for CBB dye. A 100 mg/L CBB solution (20 mL) is pipetted into an Erlenmeyer flask and adjusted to pH 5 with 0.1 M HCl. Then, 0.02 g of HAp is added to the dye solution. The mixture is stirred at 180 rpm for 4 h at 25 °C. The mixture is then separated by centrifugation (20 min, 4000 rpm), and the absorbance of the filtrate is measured using a UV-vis spectrophotometer at λ_{max} 587 nm. The same procedure is applied to HAp 1, HAp 2, HAp 4, HAp 5, HAp 6, and HAp 7. In previous studies, pH variations have been carried out to investigate their effect on the adsorption of CBB by hydroxyapatite [10]. In acidic conditions, pH = 5 is the optimum pH for active adsorption sites on the HAp made, and the adsorption capacity is excellent. It is estimated that when pH = 5, the number of active adsorption sites is the largest and the adsorption capacity is optimal. The pH value of 5 is optimal, so all experiments in this study were carried out at a pH value of 5. Adsorption capacity is then calculated for each HAp [10].

Determination of CBB adsorption isotherms

The adsorption isotherm for CBB is determined by pipetting 20 mL of a 500 mg/L CBB solution, then adjusting the pH 5. Then, 0.02 g of HAp are added to the solution. The mixture is stirred for 4 h. Afterward, the mixture is filtered, and the absorbance of the filtrate is measured at 587 nm. The same procedure is followed for CBB concentrations of 200, 300, 400, and 600 mg/L [10].

Determination of CBB adsorption kinetics

The adsorption kinetics of CBB are determined by pipetting 20 mL of a 100 mg/L CBB solution into an Erlenmeyer flask and adjusting the pH to 5. Then, 0.02 g of HAp 4 are added to the dye solution. The mixture is stirred for 60, 120, 180, 240, and 300 min. Afterward, the mixture is filtered, and the absorbance of the filtrate is measured at 587 nm [10].

In this study, the adsorption data were analyzed using both kinetic and isotherm models to understand the mechanism and capacity of the adsorption process. The kinetic models applied include the pseudo-first-order

Table 1. Precursor concentrations

HAp	HAp		Additives	
	CaO (g)	$Na_2HPO_4{\cdot}12H_2O$ (g)	Urea (g/L)	Sodium citrate (g/L)
HAp 1	1.1	4.1899	0	0
HAp 2	1.1	4.1899	30	0
HAp 3	1.1	4.1899	30	0.1
HAp 4	1.1	4.1899	30	0.2
HAp 5	1.1	4.1899	30	0.3
HAp 6	1.1	4.1899	30	0.4
HAp 7	1.1	4.1899	30	0.5

and pseudo-second-order models used to determine the rate and potential controlling steps of the adsorption process. For equilibrium studies, the Langmuir and Freundlich isotherm models were employed to evaluate the adsorption behavior and surface characteristics of the adsorbent. The best-fitting model was selected based on the correlation coefficient (R^2) and other relevant parameters such as the maximum adsorption capacity (q_m), Langmuir constant (K_L), and Freundlich constants (K_F and n). Additionally, statistical analysis was performed using regression analysis to assess the goodness-of-fit of each model. The model with the highest R^2 value and logical parameter range was considered to represent the experimental data most accurately.

Reusability

The reusability process involves pipetting 20 mL of a 100 mg/L CBB solution into an Erlenmeyer flask and adjusting the pH to 5. Then, 0.02 g of HAp are added to the CBB solution. The mixture is stirred for 120 min. The mixture is then filtered, and the filtrate is analyzed using a UV-vis spectrophotometer. The HAp is regenerated by shaking it in a 0.1 M NaOH solution for 12 h at 180 rpm to remove the dye solution, then washed with distilled water and dried. The HAp is recontacted with CBB solution through several cycles [10].

■ RESULTS AND DISCUSSION

Analysis of HAp without and with Additives

In this study, blood cockle shells were used as the calcium source for HAp synthesis, employing the sol-gel method. The resulting product is white powder, as shown in Fig. 1. HAp synthesis used Ca from CaO powder derived from blood cockle shells and phosphate from $Na_2HPO_4{\cdot}12H_2O$. CaO powder weighed 1.1 g and dissolved in CH_3COOH. This process aims to dissolve CaO into $Ca(CH_3COO)_2$. Stirring was done for 30 min to obtain a homogeneous solution. The reaction is as in Eq. (1);

$$CaO_{(s)} + 2CH_3COOH_{(aq)} \rightarrow Ca(CH_3COO)_{2(aq)} + H_2O_{(l)} \quad (1)$$

Then 10 M NaOH was added to the $Ca(CH_3COO)_2$ solution until pH 11 was reached, which is the optimum pH for forming HAp sol. $Na_2HPO_4{\cdot}12H_2O$ was then added. The reaction for forming HAp is as in Eq. (2);

$$10Ca(CH_3COO)_{2(l)} + 6(Na)_2HPO_4 \cdot 12H_2O_{(l)} + 8NaOH_{(l)} \rightarrow Ca_{10}(PO_4)_6(OH)_{2(s)} + 20CH_3COONa_{(aq)} + 18H_2O_{(l)} \quad (2)$$

As shown in Fig. 1, synthesized HAp 1–7 were obtained as a fine white powder. During synthesis, the HAp with additives tends to be hygroscopic due to the water-absorbing properties of urea and sodium citrate. Therefore, ethanol and distilled water were used to dissolve the additives present in the final HAp product. Higher concentrations of sodium citrate result in more ethanol and distilled water being used for washing the HAp.

HAp was synthesized from blood cockle shells. Based on previous research, the blood cockle shells have the main content of $CaCO_3$ as a source of calcium oxide. The results showed that %CaO content in blood cockle shells was 98% [8]. Blood cockle shells offer several advantages compared to other calcium sources such as limestone or bovine bone: they are abundant, low-cost, and derived from fishery waste, thus supporting environmental sustainability [14]. Moreover, their high purity ($CaCO_3$ content) and porous structure make them effective precursors for HAp synthesis [12]. The material was synthesized using the sol-gel method from blood shells as a source of CaO and $Na_2HPO_4{\cdot}12H_2O$ as a source of phosphate. Both precursors were mixed to form calcium phosphate, followed by the addition of

Fig 1. Results of HAp 1–7

additives, sodium citrate and urea. In the solution, urea can thermally hydrolyze to produce NH_3 and CO_2. NH_3 increases the pH of the solution, which can aid in the nucleation of HAp. Sodium citrate acts as a chelating agent, binding Ca^{2+} ions through its carboxylate groups,forming complexes that prevent the formation of large particles and help control particle size and distribution during gel formation. The amino groups (NH_2) of urea can interact with the carboxylate groups of sodium citrate (COO^-) through hydrogen bonds or electrostatic interactions [10,13].

Hydrolysis and condensation reactions cause small particles to aggregate into a three-dimensional network (gel) during the sol-gel process. Urea and sodium citrate help control the size and homogeneity of the HAp particles formed in the gel. The urea-sodium citrate-Ca^{2+} complex serves as nucleation sites, absorbing OH^- and PO_4^{3-} ions from the solution. This aids in the growth of HAp crystals around the nucleation sites. If there is an excess of Ca^{2+} ions, the formation of HAp is limited by the number of chelating sites on urea and sodium citrate, ultimately constraining the size of the formed HAp [15].

The sodium citrate concentration changes the HAp morphology. More uniform and smaller particles are formed at higher concentrations owing to greater Ca^{2+} chelation which retards crystal growth and agglomeration. With the rise in pH, urea promotes fine particle formation through enhanced NH_3 release and nucleation, which improves surface area and adsorption. On the other hand, excessive sodium citrate could lead to oversaturation of the chelating agent, inhibiting crystallization [16]. The sol-gel method has distinct advantages over wet precipitation and hydrothermal techniques, such as enhanced particle size and morphology control, lower energy consumption, and uncomplicated equipment. These advantages highlight its practicality and scalability for synthesizing HAp from bio-waste materials like blood cockle shells [17].

FTIR Analysis

FTIR analysis aims to identify functional groups through absorption peaks and molecular interactions involved in HAp synthesis. The FTIR spectra for HAp 1–7 derived from blood cockle shells are shown in Fig. 2.

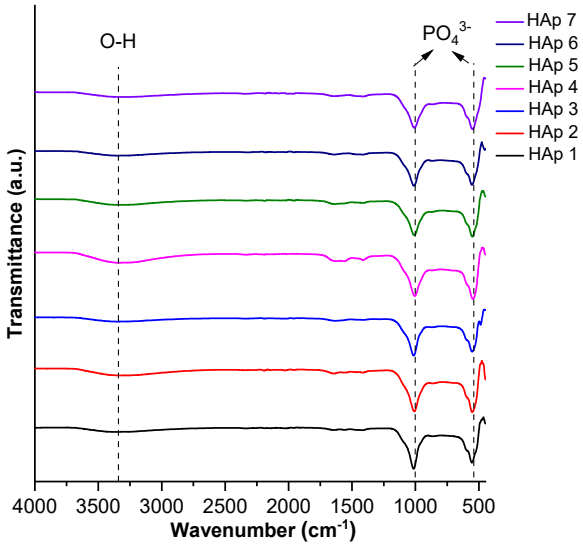

Fig 2. FTIR spectra of HAp 1–7

Fig. 2 shows the stretching of O–H corresponds to broad absorption bands at 3346 cm^{-1} whereas the sharp bands at around 1005 and 545 cm^{-1} contain the PO_4^{3-} which is also HAp, so these do confirm the existence of HAp [18]. Moreover, the FTIR spectrum of CaO obtained from raw blood cockle shells did not show these peaks, verifying that the HAp transformation was successful. The resemblance of HAp 1–7 spectra and other spectra presented in earlier studies showcases the successful attainment of Hap [10]. Changes in the peak intensity are due to sodium citrate, urea, or other factors affecting the crystallinity and morphology of the particle. These results also demonstrate that the synthesis of HAp using the sol-gel method is effective because no carbonate peaks are observed at 1415 cm^{-1}. Fig. 2 shows no significant interaction between HAp and additives because urea and sodium citrate are dissolved with ethanol and distilled water. Additives do not significantly affect the functional groups of HAp but tend to modify the morphology of HAp during the synthesis process [10].

SEM-EDS Analysis

SEM-EDS analysis was conducted on samples HAp 1, 2, 4, and 7. Fig. 3 presents the SEM-EDS results for samples HAp 1, 2, 4, and 7 at 5,000× magnification. The images reveal that the HAp particles are irregular and exhibit agglomeration, which is attributed to the addition

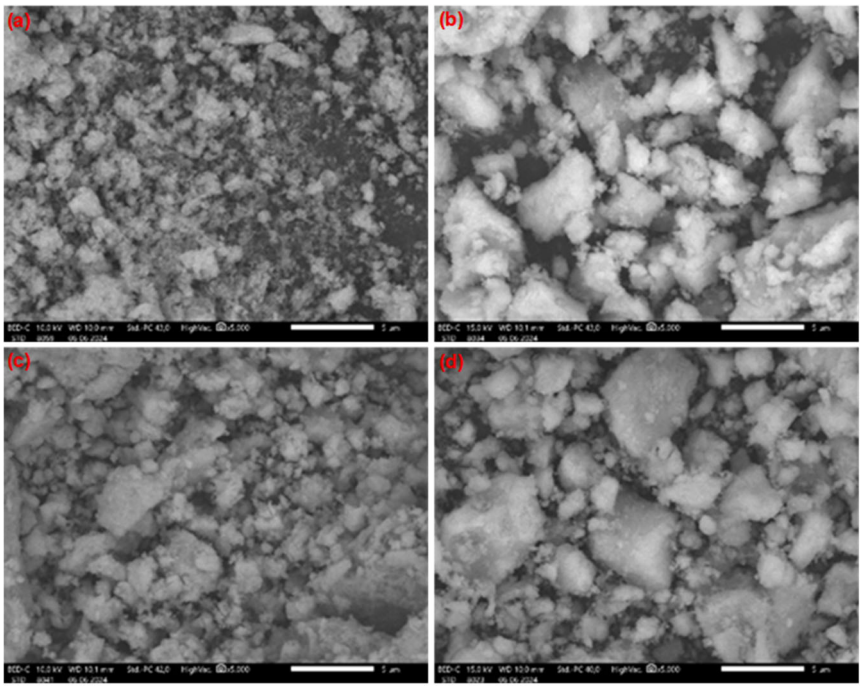

Fig 3. SEM images at 5,000× magnification: (a) HAp 1, (b) HAp 2, (c) HAp 4, and (d) HAp 7

of sodium citrate and urea. Previous study has reported that these additives lead to uneven distribution and the formation of clusters [19]. EDS results confirm the presence of HAp, indicated by the elements Ca, P, and O with a Ca/P ratio of 1.28. This value is close to the typical Ca/P ratio for HAp, which is 1.67. Previous research shows HAp can be formed with a Ca/P ratio between 1.2 and 2.0 [20]. The EDS spectrum for HAp 4 is shown in Fig. 4.

Particle size measurements were performed using ImageJ software. Fig. 5 displays the particle size distribution for HAp 2, 4, and 7. The particle size range for HAp 2, 4, and 7 is between 0.1 and 7 μm, with average sizes of 2.13, 1.16, and 1.88 μm, respectively. The smallest particle size was obtained for sample HAp 4 with 30 g/L urea and 0.2 g/L sodium citrate. This indicates the effect of urea and sodium citrate on the particle size of HAp. The particle size can influence the stability of the adsorbent material and its ability to be regenerated (returned to its original state after adsorption). Smaller particles are more prone to agglomeration or structural changes during the regeneration process to adsorption [21].

The addition of urea and sodium citrate plays an essential role in controlling the particle size during the synthesis process. Urea acts as a pH-regulating agent that slowly decomposes into NH_3 and CO_2, gradually increasing the pH. This process promotes more controlled nucleation, resulting in more small particle nuclei due to limited crystal growth. On the other hand, sodium citrate acts as a chelating agent that binds Ca^{2+}, forming citrate-metal complexes that inhibit the direct

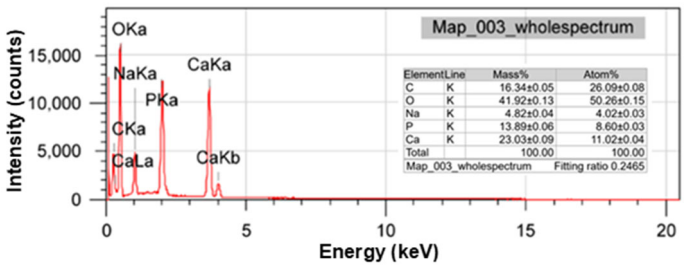

Fig 4. EDS spectrum of HAp 4

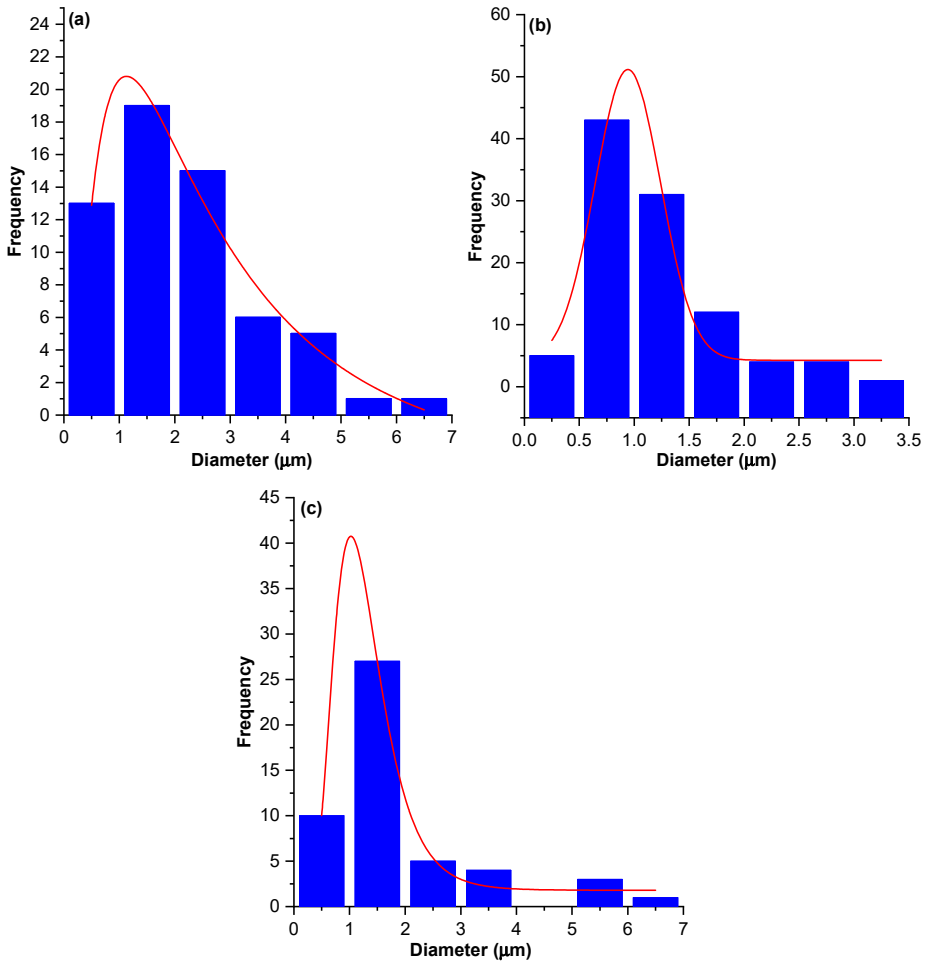

Fig 5. Particle size distribution: (a) HAp 1, (b) HAp 4, and (c) HAp 7

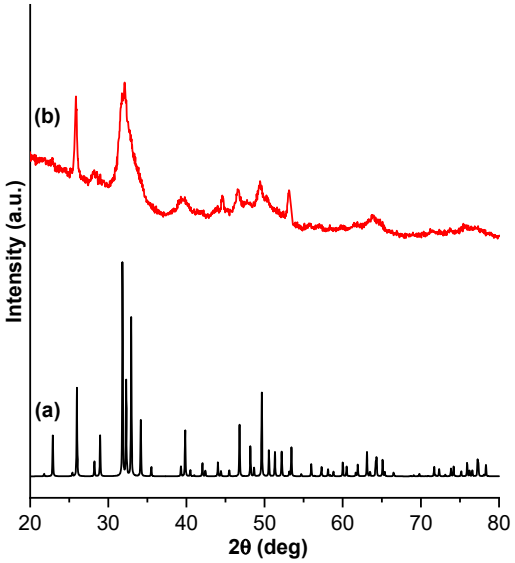

Fig 6. XRD profile of (a) standard Hap and (b) HAp 4

release of free ions into the solution. This slows the crystal growth rate and allows smaller and more uniform particles to form. However, when the sodium citrate concentration is too high, the number of free metal ions becomes very small, inhibiting initial nucleation, and only a few nuclei form. As a result, the available ions will contribute more to the growth of existing particles rather than forming new nuclei, resulting in larger particles, even exceeding 4 μm. In addition, excess sodium citrate can cause steric or bridging effects between particles that accelerate aggregation, significantly increasing the average particle size [10,13].

XRD Analysis

The diffraction pattern of HAp derived from blood clam shells shows diffraction peaks consistent with the HAp standard diffraction (ICSD #157481) as shown in Fig. 6(a). The XRD spectrum for HAp 4 indicates that

the crystallinity of HAp decreases with the addition of sodium citrate and urea. The crystal size was calculated using the Scherrer equation, resulting in a crystal size of 24.55 nm for HAp 4. Fig. 6(b) demonstrates the broadening of the diffraction peaks for HAp 4, which is attributed to the influence of adding sodium citrate and urea. The broadening of the diffraction peaks for HAp 4 indicates a reduction in crystallinity, which is advantageous for adsorption applications [10].

SAA Analysis

The SAA analysis aims to determine the specific surface area of HAp 4 using the Brunauer-Emmett-Teller (BET) method. This method employs N_2 gas adsorption/desorption to determine the surface area. The SAA analysis results showed that the surface area of HAp 4 is 107.691 m^2/g, with a pore size of 12.55 nm and a pore volume of 0.36 cm^3/g. The large surface area, pore size, and pore volume indicate a high adsorption capacity due to the increased number of active sites for interaction with the molecules to be adsorbed [22]. Table 2 shows the crystallite size, surface area, and particle size of HAp with various methods and conditions.

CBB Adsorption Capacity

The adsorption capacity represents the amount of adsorbate that can accumulate on the adsorbent's surface. The adsorbents used are HAp 1–7. The optimal conditions to determine the adsorption capacity of CBB by HAp are an adsorbent mass of 0.02 g, a solution pH of 5, and a contact time of 240 min [10]. The adsorption capacity test results for HAp can be seen in Table 3.

Table 3 shows that the highest adsorption capacity is found in HAp 4, at 96.6059 mg/g. In Fig. 5 and Table 3, it can be seen that particle size affects the adsorption capacity; the smaller the particle size, the higher the adsorption capacity. HAp 4 exhibits optimal adsorption, with a balance between the number of available active sites and their accessibility (interaction between the adsorbent and adsorbate).

HAp 4 demonstrated the most significant CBB adsorption capacity of 96.6059 mg/g, which can be attributed to its smaller particle size of 1.16 μm, higher surface area of 107.691 m^2/g, fewer crystalline structures, and active functional groups as determined by FTIR. The use of sodium citrate and urea during the synthesis process increased the uniformity and porosity of the particles, thus enhancing the interactions between the adsorbate and the adsorbent. The adsorption capacity of an adsorbent is determined by adsorption parameters, including pH, temperature, solution concentration, adsorbent mass, pore structure of the adsorbent, surface area of the adsorbent, contact time, and particle size of the adsorbent [25].

CBB Isotherm Analysis

The adsorption isotherm analysis of CBB was performed using HAp 4. Adsorption isotherms represent the equilibrium relationship between the concentration of adsorbate in the solution and its concentration within the particles on the adsorbent [3]. Adsorption isotherms can indicate the type of adsorbate

Table 3. Adsorption capacity of CBB dye by HAp

Sample	q_e (mg/g)	%Adsorption
HAp 1	51.4153	51.4153
HAp 2	88.2161	88.2161
HAp 3	95.4831	95.4831
HAp 4	**96.6059**	**96.6059**
HAp 5	94.4237	94.4237
HAp 6	92.9619	92.9619
HAp 7	92.6441	92.6441

Table 2. HAp characteristics by various methods

Synthesis method	Crystallite size (nm)	Particle size (μm)	Surface area (m^2/g)	Synthesis conditions	Reference
Sol-gel	24.55	1.87 (HAp 4)	107.69	pH 11; 30 g/L urea; 0.2 g/L sodium citrate	This study
Wet precipitation	26.40	0.953	90.15	pH 10; calcination 800 °C for 4 h	[22]
Precipitation + calcination	19.08	0.0571	105.80	pH 7–11; calcination 800 °C for 4 h	[23]
Precipitation	26–38	0.3	Not reported	Calcination 800 °C, 4 h; no additives	[24]

layer formed on the adsorbent's surface. In this study, HAp 4 was used as the adsorbent with varying concentrations of CBB dye at 200, 300, 400, 500, and 600 mg/L. The Langmuir and Freundlich isotherms are the adsorption models used in this study.

Fig. 7 shows the linear isotherm graphs for Langmuir and Freundlich for the adsorption of CBB with HAp 4. In Fig. 7., a linear relationship is observed for the adsorption capacity (q_m) from the intercept value and the Langmuir isotherm constant (K_L) from the slope value. From the linear equation, the adsorption intensity (n) value is also obtained from the slope, and the Freundlich adsorption capacity (K_F) value is derived from the intercept. Based on Fig. 7., the CBB adsorption isotherms using HAp 4 were obtained. The Langmuir isotherm had an R^2 value of 0.9775, and the Freundlich isotherm had an R^2 value of 0.8974. Thus, the CBB adsorption process follows the Langmuir isotherm equation, as the R^2 value for the Langmuir isotherm is higher than that for the Freundlich isotherm.

The adsorption of CBB onto HAp was modeled using the Langmuir isotherm, and the results supported high R^2 for the model, which indicates that this model was suitable for describing the adsorption process. Moreover, CBB molecules' size and net charge facilitate surface interactions which reinforce monolayer formation, adhering to the Langmuir model's underlying assumptions of uniform surface adsorption capped at finite q_m, without intermolecular dependencies. Freundlich, in contrast, pertains to isotherms where adsorption takes place at heterogeneous surfaces. This study, however, diverges from conventional accepted norms due to observing n, the Freundlich constant, exceeding 10, suggesting a weak empirical correlation (desired ranges $1 < n < 10$) [3]. Consequently, these data indicate that at both theoretical and empirical levels, CBB adsorption onto HAp complies with the Langmuir model rather than the Freundlich model, endorsing the adsorption isotherm's applicability.

These results align with other past works that pointed out the applicability of the Langmuir model to dye adsorption systems with HAp served as an adsorbent. For instance, Mobarak et al. [26] showed that HAp synthesized from eggshell waste showed very high efficiency in adsorbing Congo red dye, and the experimental data was best represented with the Langmuir isotherm.

Adsorption Kinetics Analysis of CBB

The adsorption kinetics analysis of CBB was conducted using HAp 4. Adsorption kinetics aim to determine the rate of adsorption occurring on the adsorbent for the adsorbate [3]. The adsorption kinetics model for CBB by HAp 4 was determined at a concentration of 100 mg/L with a mass of HAp 4 of 0.02 g and contact time variations of 1, 2, 3, 4, and 5 h. This study used two types of kinetics models: pseudo-first-order and pseudo-second-order. Fig. 8 shows the

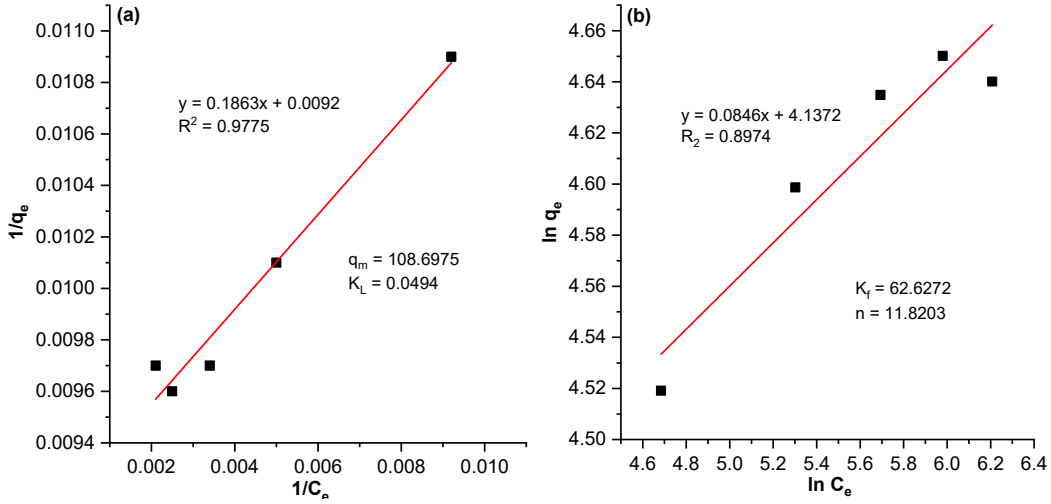

Fig 7. Linear isotherm graphs of (a) Langmuir and (b) Freundlich for the adsorption of CBB with HAp 4

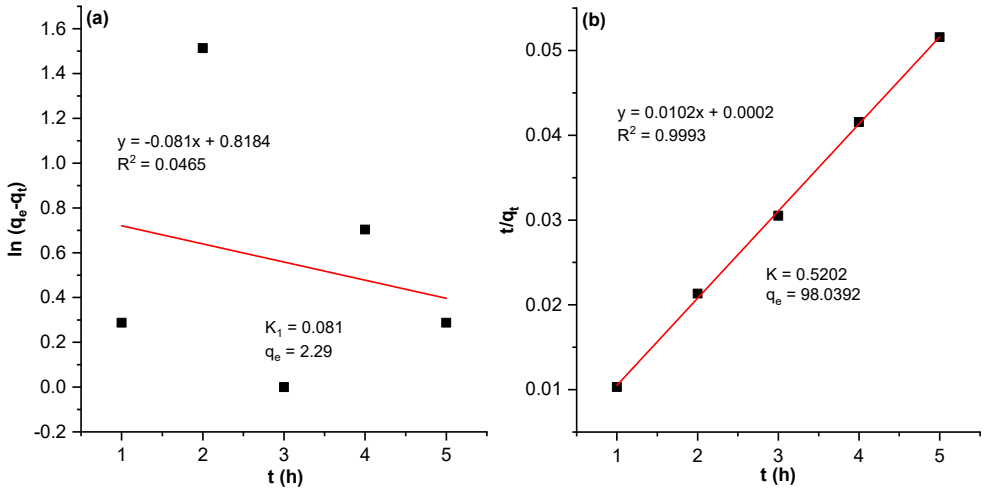

Fig 8. Linear kinetic (a) pseudo-first-order and (b) pseudo-second-order models for CBB adsorption by HAp 4

linear kinetic model graphs of pseudo-first-order and pseudo-second-order for the adsorption of CBB by HAp 4. It is shown that the adsorption kinetics of CBB using HAp 4 follow the pseudo-second-order kinetics model, indicated by a higher R^2 of 0.9993 compared to the pseudo-first-order model. Previous study also showed a pseudo-second-order kinetic model for rhodamine B adsorption, indicating that chemical interactions occurred during the adsorption of rhodamine B dye using HAp from cuttlefish bone [20]. The pseudo-second-order model demonstrates that the availability of active sites on the surface of HAp controls the adsorption process. The HAp surface has a complex crystalline structure with various adsorption sites, such as PO_4^{3-} and OH^- sites. These groups can form complex bonds with dye molecules, enhancing the adsorption process. The dye molecules can interact with these functional groups on the HAp surface, creating stable complexes that are difficult to desorb [3].

Reusability Analysis

The reusability analysis of HAp 4 was conducted for CBB adsorption. Reusability is a crucial aspect of adsorbents, as it can reduce costs and enhance process efficiency. The desorption agents used for HAp 4 were NaOH and HCl [10]. These desorption agents function to remove contaminants adsorbed on the adsorbent. The adsorption cycle of CBB by HAp 4 is illustrated in Fig. 9.

The reusability of CBB adsorption by HAp 4 was tested using a concentration of 100 mg/L with the optimum pH and stirred for 2 h. Fig. 9 indicates HAp 4 potential to use adsorb CBB effectively until five cycles. The decrease in adsorption percentage is due to the saturation of active sites on the adsorbent by dye molecules with each cycle. Additionally, the adsorbent begins to degrade under extreme pH conditions and experiences blockage in the pores and active sites on its surface [21]. Thus, it can be concluded that HAp 4 performs well in reducing CBB dye waste in aqueous solutions because HAp has excellent adsorption capacity and stability.

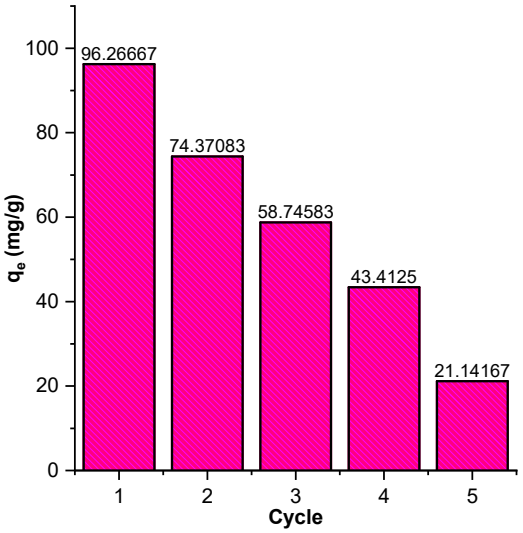

Fig 9. Adsorption cycle of CBB by HAp 4

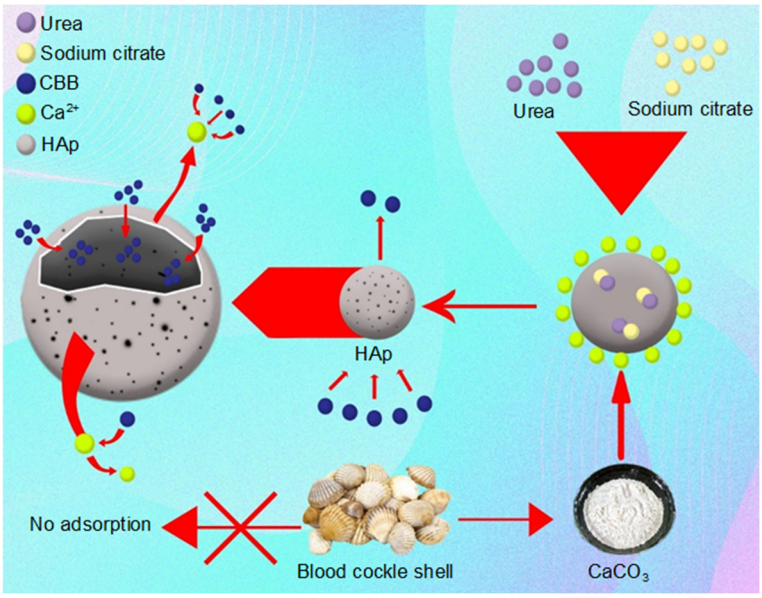

Fig 10. Proposed mechanism of CBB adsorption by HAp

Proposed Adsorption Mechanism of CBB by HAp

The proposed adsorption mechanism of CBB by Hap is visualized in Fig. 10. HAp exhibits high adsorption capacity due to its large surface area and numerous active sites. HAp interacts with dyes through ionic bonds and electrostatic interactions [10]. CBB is an anionic molecule, allowing it to interact with Ca^{2+} ions present on the surface of HAp. Sodium citrate can enhance the dispersibility of HAp in solution, thereby making more active sites available for interaction with CBB. Urea can increase the number of pores and improve the specific surface area of HAp [11,22].

Under acidic conditions, the surface of HAp can become positively charged due to increased protonation. The CBB molecule contains negatively charged sulfonate groups ($-SO_3^-$) [27]. The positive charge on HAp attracts the negative charge on CBB, strengthening adsorption through electrostatic attraction. Additionally, strong ionic bonds form between Ca^{2+} on HAp and $-SO_3^-$ on CBB, further reinforcing adsorption. Hydrogen bonds can also form during adsorption. These occur between hydrogen bond donors and acceptors, specifically atoms with lone electron pairs and hydrogen atoms attached to electronegative atoms. HAp contains groups that can act as hydrogen bond donors or acceptors. Functional groups on CBB, such as sulfonates, will participate in hydrogen bonding. In acidic conditions, protonation of certain groups on HAp can enhance their ability to form hydrogen bonds with functional groups on CBB [28].

Adsorption involves ion exchange, where ions from the solution are exchanged with ions on the surface of the adsorbent. Ca^{2+} ions on the surface of HAp can exchange with other groups on CBB, allowing CBB to adhere through ion exchange in acidic conditions [10]. The combination of various interactions (electrostatic, ionic, hydrophobic, hydrogen bonding, and ion exchange) and the influence of acidic conditions enables HAp, when modified with sodium citrate and urea, to exhibit high adsorption capacity for CBB.

■ CONCLUSION

HAp derived from blood clam shells with sodium citrate and urea was successfully synthesized using the sol-gel method. The concentration of sodium citrate affects the adsorption capacity of HAp, with HAp containing 0.2 g/L sodium citrate and 30 g/L urea (HAp 4) showing optimal results in adsorbing CBB. FTIR analysis indicated the presence of O–H and PO_4^{3-} groups, while XRD confirmed the standard HAp pattern with peak broadening. SEM-EDS revealed agglomeration and irregular particles with a Ca/P ratio of 1.28. SAA analysis showed a surface area of 107.2841 m^2/g, a pore size of 12.55 nm, and a pore

volume of 0.36 cm^3/g. HAp 4 followed the Langmuir isotherm and pseudo-second-order kinetic models and demonstrated good reusability over five cycles. Therefore, the sodium citrate and urea additives influence the morphology of HAp, enhancing its adsorption capacity, and HAp 4 is the most effective adsorbent for reducing CBB waste.

■ ACKNOWLEDGMENTS

This research was supported by *Kementerian Pendidikan, Kebudayaan, Riset, dan Teknologi, Republik Indonesia*, Universitas Andalas, *Lembaga Penelitian dan Pengabdian kepada Masyarakat*, 2024 (grant number: 210/UN16.19/PT.01.03/PSS/2024).

■ CONFLICT OF INTEREST

The authors have no conflict of interest.

■ AUTHOR CONTRIBUTIONS

Novesar Jamarun collected the experimental data, Dhea Rahmanda Putri and Vivi Sisca drafted the manuscript, and Novesar Jamarun and Upita Septiani developed the idea and corrected the manuscript. All authors read and approved the final manuscript.

■ REFERENCES

[1] Ramamurthy, K., Priya, P.S., Murugan, R., and Arockiaraj, J., 2024, Hues of risk: Investigating genotoxicity and environmental impacts of azo textile dyes, *Environ. Sci. Pollut. Res.*, 31 (23), 33190–33211.

[2] Saravanan, S., Carolin C, F., Kumar, P.S., Chitra, B., and Rangasamy, G., 2022, Biodegradation of textile dye Rhodamine-B by *Brevundimonas diminuta* and screening of their breakdown metabolites, *Cemosphere*, 308 (Pt. 1), 136266.

[3] Ata, S., Imran Din, M., Rasool, A., Qasim, I., and Ul Mohsin, I., 2012, Equilibrium, thermodynamics, and kinetic sorption studies for the removal of Coomassie brilliant blue on wheat bran as a low-cost adsorbent, *J. Anal. Methods Chem.*, 2012 (1), 405980.

[4] Amenaghawon, A.N., Anyalewechi, C.L., Darmokoesoemo, H., and Kusuma, H.S., 2022, Hydroxyapatite-based adsorbents: Applications in sequestering heavy metals and dyes, *J. Environ. Manage.*, 302 (Pt. A), 113989.

[5] Jamarun, N., Caniago, S., Septiani, U., Prasejati, A., Wulandari, W., and Amirullah, T.Y., 2024, Synthesis and characterization of hydroxyapatite composite from cuttlebone (*Sepia* sp.) with chitosan via *in situ* as antibacterial, *ChemistrySelect*, 9 (3), e202303514.

[6] Wang, H., Yan, K., Xing, H., Chen, J., and Lu, R., 2021, Effective removal of Cu^{2+} from aqueous solution by synthetic abalone shell hydroxyapatite microspheres adsorbent, *Environ. Technol. Innovation*, 23, 101663.

[7] Trakoolwannachai, V., Kheolamai, P., and Ummartyotin, S., 2019, Characterization of hydroxyapatite from eggshell waste and polycaprolactone (PCL) composite for scaffold material, *Composites, Part B*, 173, 106974.

[8] Jamarun, N., Trycahyani, N.A., Arief, S., Septiani, U., and Sisca, V., 2023, Synthesis of hydroxyapatite-polyethylene glycol with *in-situ* method using calcium oxide from blood shells (*Anadara granosa*), *Indones. J. Chem.*, 23 (3), 618–626.

[9] Dewi, N., Rahmah, R.A., Wardhana, A.S., Puspitasari, D., Wasiaturrahmah, Y., and Gustiono, D., 2025, Remineralizing potential of natural hydroxyapatite from snakehead (*Channa striata*) fish bone on remineralization of primary teeth enamel: An *in vitro* study, *Eur. J. Gen. Dent.*, 14 (1), 11–19.

[10] Wang, H., Xing, H., Yan, K., Han, D., and Chen, J., 2022, Oyster shell derived hydroxyapatite microspheres as an effective adsorbent for remediation of Coomassie brilliant blue, *Adv. Powder Technol.*, 33 (2), 103425.

[11] Jin, X., Zhuang, J., Zhang, Z., Guo, H., and Tan, J., 2015, Hydrothermal synthesis of hydroxyapatite nanorods in the presence of sodium citrate and its aqueous colloidal stability evaluation in neutral pH, *J. Colloid Interface Sci.*, 443, 125–130.

[12] Sun, Y., Wang, Y., Ji, C., Ma, J., and He, B., 2024, The impact of hydroxyapatite crystal structures and protein interactions on bone's mechanical properties, *Sci. Rep.*, 14 (1), 9786.

[13] Fitri, R.A., Wirakusuma, A., Aulia, M.P., Dewi, R., and Arahman, N., 2024, Synthesis and characterization of carbonate-substituted hydroxyapatite from eggshell waste using urea and diammonium hydrogen phosphate, *Ann. Chim.*, 48 (6), 871–878.

[14] Hart, A., 2020, Mini-review of waste shell-derived materials' applications, *Waste Manage. Res.*, 38 (5), 514–527.

[15] Martins, M.A., Santos, C., Almeida, M.M., and Costa, M.E.V., 2008, Hydroxyapatite micro- and nanoparticles: Nucleation and growth mechanisms in the presence of citrate species, *J. Colloid Interface Sci.*, 318 (2), 210–216.

[16] Jokic, B., Tanaskovic, D., Jankovic-Castvan, I., Drmanic, S., Petrovic, R., and Janackovic, D., 2007, Synthesis of nanosized calcium hydroxyapatite particles by the catalytic decomposition of urea with urease, *J. Mater. Res.*, 22 (5), 1156–1161.

[17] Soreto, S., Devesa, S., Carvalho, S., and Benzarti, Z., 2025, "Sol-Gel Synthesis of Hydroxyapatite: Applications, Methods, and a Case Study" in *Sol-Gel - A Versatile and Wide Technology*, IntechOpen, Rijeka, Croatia.

[18] Musa, B., Raya, I., and Natsir, H., 2016, Synthesis and characterizations of hydroxyapatite derived blood clam shells (*Anadara granosa*) and its potency to dental remineralizations, *Int. J. Appl. Chem.*, 12 (4), 527–538.

[19] Pinchuk, N.D., Sobierajska, P., Szyszka, K., Bezkrovnyi, O., and Wiglusz, R.J., 2024, Preparation of nanohydroxyapatite with diverse morphologies and optimization of its effective aqueous colloidal dispersions for biomedical applications, *Ceram. Int.*, 50 (15), 27426–27435.

[20] Jamarun, N., Prasejati, A., Zulhadjri, Z., Caniago, S., Amirullah, T.Y., Wulandari, W., and Sisca, V., 2024, Effect of chitosan concentration on hydroxyapatite/chitosan composite synthesis using the in-situ method as a dye adsorbent, *Kuwait J. Sci.*, 51 (4), 100252.

[21] Yang, H., and Wang, Y., 2016, Morphology control of hydroxyapatite microcrystals: Synergistic effects of citrate and CTAB, *Mater. Sci. Eng., C*, 62, 160–165.

[22] Nagasaki, T., Nagata, F., Sakurai, M., and Kato, K., 2017, Effects of pore distribution of hydroxyapatite particles on their protein adsorption behavior, *J. Asian Ceram. Soc.*, 5 (2), 88–93.

[23] Mtavangu, S.G., Mahene, W., Machunda, R.L., van der Bruggen, B., and Njau, K.N., 2022, Cockle (*Anadara granosa*) shells-based hydroxyapatite and its potential for defluoridation of drinking water, *Results Eng.*, 13, 100379.

[24] Sinurat, E., Dewi, F.R., Fransiska, D., and Nurbayasari, R., 2022, Synthesis and characterization of hydroxyapatite of cockle shells (*Anadara granosa*) originated from Indonesia through precipitation method, *IOP Conf. Ser.: Earth Environ. Sci.*, 1118 (1), 012035.

[25] Wu, J., Yang, J., Huang, G., Xu, C., and Lin, B., 2020, Hydrothermal carbonization synthesis of cassava slag biochar with excellent adsorption performance for Rhodamine B, *J. Cleaner Prod.*, 251, 119717.

[26] Bin Mobarak, M., Pinky, N.S., Chowdhury, F., Hossain, M.S., Mahmud, M., Quddus, M.S., Jahan, S.A., and Ahmed, S., 2023, Environmental remediation by hydroxyapatite: Solid state synthesis utilizing waste chicken eggshell and adsorption experiment with Congo red dye, *J. Saudi Chem. Soc.*, 27 (5), 101690.

[27] Thamer, B.M., Aldalbahi, A., Moydeen A.M., El-Hamshary, H., Al-Enizi, A.M., and El-Newehy, M.H., 2019, Effective adsorption of Coomassie brilliant blue dye using poly(phenylene diamine)grafted electrospun carbon nanofibers as a novel adsorbent, *Mater. Chem. Phys.*, 234, 133–145.

[28] Joe Pushba Shini, J., Joy Prabu, H., Felix Sahayaraj, A., Johnson, I., Thaninayagam, E., Gopi, R.R., and Snowlin, V., 2024, Synthesis of hydroxyapatite (HAp) from eggshells via thermal decomposition method for the application of dye adsorption, *J. Indian Chem. Soc.*, 101 (10), 101321.